Nonequilibrium Heating in LHCII Complexes Monitored by Ultrafast Absorbance Transients†

Vidmantas Gulbinas,‡ Renata Karpicz,‡ Gyözö Garab,§ and Leonas Valkunas*,‡,||

Institute of Physics, Savanoriu 231, LT-02300 Vilnius, Lithuania, Institute of Plant Biology, Biological Research Center of the Hungarian Academy of Sciences, P.O. Box 521, H-6701 Szeged, Hungary, and Department of Theoretical Physics, Faculty of Physics, Vilnius University, Sauletekio 9, build. 3, LT-10222 Vilnius, Lithuania

Received January 10, 2006; Revised Manuscript Received June 16, 2006

ABSTRACT: Evidence of nonequilibrium local heating in transient spectra of LHCII, the main light-harvesting complex of plants, was studied by using various excitation intensities over a wide temperature range, from 10 K to room temperature. No obvious manifestation of local heating was found at room temperature, whereas at 10 K, the local heating effect is discernible when more than 10 excitons per LHCII trimer per pulse are generated. Under these conditions, a major part of the excitation energy is converted into heat as a result of exciton−exciton annihilation. Initially, the heat energy is allocated on chlorophyll *a* molecules, reaching hundreds of degrees at the highest excitation intensities, which correspond to almost 100 excitons per trimer generated by a single excitation pulse. The decay of the nonequilibrium temperature is characterized well by two exponentials. The initial phase of cooling, which is most likely caused by the spreading of heat over the protein, corresponds to a characteristic time constant of ∼20 ps. Later, the cooling rate decelerates to approximately 200 ps and is related to heat transfer to the solvent.

Two photosystems, PSI[1] and PSII, coupled in the so-called Z-scheme of electron transfer, are basic constituents of the photosynthetic apparatus of cyanobacteria, algae, and green plants. In higher plants, the main chlorophyll *a*/*b* light-harvesting complex of PSII, LHCII, in addition to its primary light-harvesting function, is also involved in a number of short- and long-term regulatory mechanisms, which respond to changes in the environmental conditions (*1*, *2*). Because of such adaptation features, plant photosynthesis may function under very different light conditions up to very high intensities. Under intense light conditions, the singlet excited state of chlorophyll *a* (Chl *a*) can be quenched non-photochemically, consequently downregulating the light-harvesting efficiency of PSII. Non-photochemical quenching contains a short-term (1−2 min) component, qE, which depends on the transmembrane ΔpH (*3*) as well as the presence of the PsbS protein (*4*) and zeaxanthin (*5*), resulting in a feedback de-excitation via a charge transfer state of the heterodimer zeaxanthin−Chl *a* complex (*6*). In general, carotenoids appear to play a special role in regulation of dissipation of the excess excitation energy in the light-harvesting antenna of PSII (*7*−*9*).

Thus, LHCII plays an active role in adjusting its own function, and in the feedback regulation of the light harvesting efficiency. Isolated LHCII complexes exhibit light-induced reversible fluorescence quenching (*10*), which can be associated with structural reorganizations (*11*, *12*). Loosely stacked lamellar aggregates of LHCII possess the ability to undergo gross light-induced reversible structural reorganizations (*13*). These reorganizations and similar transients in thylakoid membranes (*14*, *15*) are approximately linearly proportional to the intensity of the photoexcitation. The effect has been ascribed to an opto-thermal mechanism, wherein localized structural changes are induced by thermal instabilities in the close vicinity of the heat dissipation (*16*, *17*). Spectroscopic and thermodynamic studies have suggested that the structural changes in thylakoids involve (i) unstacking of membranes followed by (ii) a lateral disorganization of the macrodomains and (iii) monomerization of the LHCII trimers (*18*, *19*). This type of elementary structural changes might occur if thermal instability is inherent in the structure around the site of heat dissipation. These reorganizations might play an important role in adaptation and photoprotection of plants under high-light conditions (*12*). Earlier, it has been shown that the de-excitation of the singlet excited state of Chl *a* molecules in light-harvesting complexes causes a substantial inflow of heat in their vicinity (*20*). Simple model calculations showed that the magnitude and temporal evolution of these thermal transients might provoke elementary structural changes (*16*, *17*). However, our knowledge concerning the site and kinetics of these heat jumps due to dissipation of photon energies is still rudimentary.

† This work was in part supported by grants from the Lithuanian State Science and Studies Foundation (C-34/2005), the Hungarian Research Fund, OTKA (T34188 and T42696), from the EU FP6 MC RTN project, INTRO2 to G.G., and the Center of Excellence Programme of EU DGXII awarded to the Biological Research Center of the Hungarian Academy of Sciences (WP17).

* To whom correspondence should be addressed. E-mail: leonas.valkunas@ff.vu.lt. Phone: +370 5 2661642. Fax: +370 5 2602317.

‡ Institute of Physics.

§ Biological Research Center of the Hungarian Academy of Sciences.

|| Vilnius University.

[1] Abbreviations: PSI, photosystem I; PSII, photosystem II; LHCII, light-harvesting complex II; Chl *a*, chlorophyll *a*; Chl *b*, chlorophyll *b*.

10.1021/bi060048a CCC: $33.50
Published on Web 07/13/2006

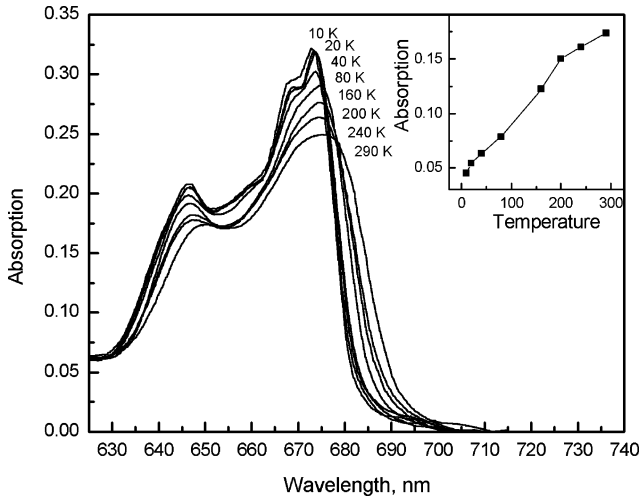

FIGURE 1: Absorption spectra of the LHCII aggregates at various temperatures. The inset shows the temperature dependence of the absorption at 682 nm.

To clarify the mechanisms and pathways of excess energy dissipation, we present particular studies of the spectral evolution caused by nonequilibrium (local) heating in LHCII aggregates under high-intensity illumination by short light pulses. Investigations were performed over a wide temperature range from 10 K to room temperature and revealed the local temperature dynamics and their influence on the spectral properties of Chl molecules.

MATERIALS AND METHODS

Aggregates of LHCII complexes were prepared as described elsewhere (*21*). Small aggregates and trimers were obtained by adding ≤0.015% (v/v) Triton X-100 to the preparation containing LHCII at 15 μg/mL Chl ($a + b$) suspended in 10 mM Tricine buffer (pH 7.8). To form a transparent sample at low temperatures, the samples were suspended in the same buffer supplemented with 67% (v/v) glycerol.

Absorption spectra were measured with the Beckman UV 5270 spectrophotometer. The absorbance of the samples in a cuvette with an optical path length of 2.5 mm was adjusted to ~0.25 at the maximum of the red absorption band. For transient absorption measurements, a pump−probe spectrometer with a 2 ps time resolution based on a 5 Hz repetition rate passively mode-locked Nd-glass laser was used. Excitation of the samples was performed by a Stokes component (624 nm), obtained from Raman scattering of the second harmonic (527 nm) of the fundamental laser radiation in ethanol. In addition, a white light continuum, generated in a water cell, was used as the probe light. The measurements were carried out in a closed cycle helium cryostat enabling cooling of the sample to 10 K.

RESULTS

Absorption spectra of LHCII aggregates in the Q_y-band region of Chl molecules exhibit two characteristic bands with some additional fine structure, which becomes more pronounced when the temperature is lowered as shown in Figure 1. The long wavelength band at 670−680 nm originates from Chl *a* absorption, while the band at ~645 nm is associated with Chl *b* absorption. However, the fine structure is attributed to specific interactions of the Chl molecules with proteins and with the carotenoid molecules and to excitonic interactions between Chl molecules. It is noteworthy that both Chl *a* and Chl *b* bands shift to longer wavelengths with temperature. The most pronounced absorption changes caused by temperature appear on the red side of the long wavelength absorption band. As indicated in the inset of Figure 1, the temperature dependence of the absorbance at 682 mn is close to linear with slight saturation evidence at higher temperatures; hence, this wavelength can be conveniently used to spectroscopically monitor the local heating effect.

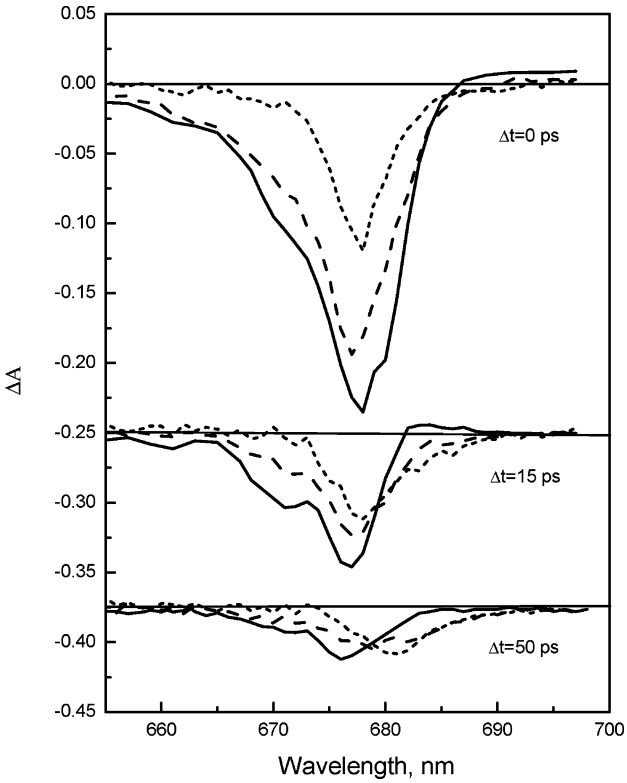

FIGURE 2: Difference absorption spectra at various delay times after excitation of the LHCII aggregates at 10 K. The 2 ps pulses of the intensity corresponding to 68 photons/trimer (—), 36 photons/trimer (− − −), and 6 photons/trimer (- - -) were used for excitation at 624 nm.

The intensity dependence of the low-temperature difference absorption spectra (ΔA) measured at different delay times is presented in Figure 2. The excitation wavelength (624 nm) is not selective for Chl *a* and Chl *b* molecules, and according to the decomposition of the LHCII absorption spectra, the extinction coefficients of the Chl *a* and Chl *b* molecules at this wavelength are comparable (*22*). Therefore, both Chl *a* and Chl *b* should equally experience excitation under our experimental conditions. However, the bleaching band in ΔA is observed only in the region of the Chl *a* optical transition. This is particularly evident at low excitation intensities, when the bleaching band involves only the absorption subband with the maximum at ~676 nm. At zero delay time, the difference absorption spectra measured at different intensities are similar in shape. However, at longer delays, the bleaching band shifts to longer wavelengths at low excitation intensities, whereas at high excitation intensities, it shifts to shorter wavelengths. The bleaching intensity at the 50 ps delay is nearly independent of the excitation

intensity, which is an indication that nonlinear relaxation, namely, exciton−exciton annihilation, is dominating and the high-intensity limit of the exciton density has already been reached.

The transient absorption kinetics at the band maximum (677 nm) and at the long wavelength slope (682 nm) measured at different temperatures and at different excitation intensities are shown in Figures 3−5. Despite a small difference between the probe wavelengths, the transient absorption kinetics at the two wavelengths exhibit very different dependencies on temperature and excitation intensity. The kinetic traces at 677 nm are almost insensitive to temperature. When the excitation intensity is increased, the relaxation kinetics during the initial 10−20 ps becomes faster as a result of exciton−exciton annihilation (see the Discussion). However, the kinetics becomes nearly independent of the excitation intensity when it exceeds 10 photons/trimer (only the kinetics at 68 photons/trimer is presented; however, the kinetics at lower intensities, but exceeding 10 photons/trimer, is identical). In contrast, the kinetics at 682 nm changes significantly with temperature and excitation intensity. At 10 K, with the lowest excitation intensity, the absorption bleaching at 682 nm increases at a rate slightly slower than the rate of temporal resolution of the setup, while the relaxation takes place on a time scale of hundreds of picoseconds. When the excitation intensity is increased, both the rise and decay kinetics become faster. At very high intensities, the light-induced absorption appears with a 10−20 ps delay.

The fraction of the excited Chl *a* molecules at a particular delay time can be estimated from the transient absorption spectrum by using the following relationship:

$$\frac{n^*}{N} = \frac{\int \Delta A(\nu)\, d\nu}{\int A(\nu)\, d\nu} \frac{\int \sigma_0\, d\nu}{\int (\sigma_0 + \sigma_{em} - \sigma^*)\, d\nu} \qquad (1)$$

where $\sigma_0(\nu)$, $\sigma_{em}(\nu)$, and $\sigma^*(\nu)$ are the absorption, emission, and excited-state absorption cross sections of the Chl *a* molecules, respectively. For estimation purposes, the spectral shapes of the cross sections were taken from the literature (see, for instance, refs *22* and *23*). The integration was performed within the 655−695 nm spectral region. For calculation of the time evolution of the excited Chl *a* molecules, the kinetics at the maximum of the bleaching band (at 677 nm), where the influence of the band shift is minimal, was used. It was assumed that ΔA at 677 nm is proportional to n^*. Kinetics of the n^*/N ratio was obtained from the normalized ΔA kinetics by using the n^*/N values for zero delay times as defined from the transient absorption spectra. Finally, the exciton number per trimer was estimated. The right axis in Figure 4 indicates these values for different excitation intensities.

DISCUSSION

Time scales for the transfer of excitons between molecules in LHCII monomers (*24*), trimers, and aggregates (*25*) are well defined by means of time-resolved pump−probe spectroscopy. Excitation transfer from Chl *b* to Chl *a* molecules at room temperature is very fast, taking place within hundreds of femtoseconds, whereas the final exciton localization at the lowest-energy sites occurs in ~5 ps (*9*).

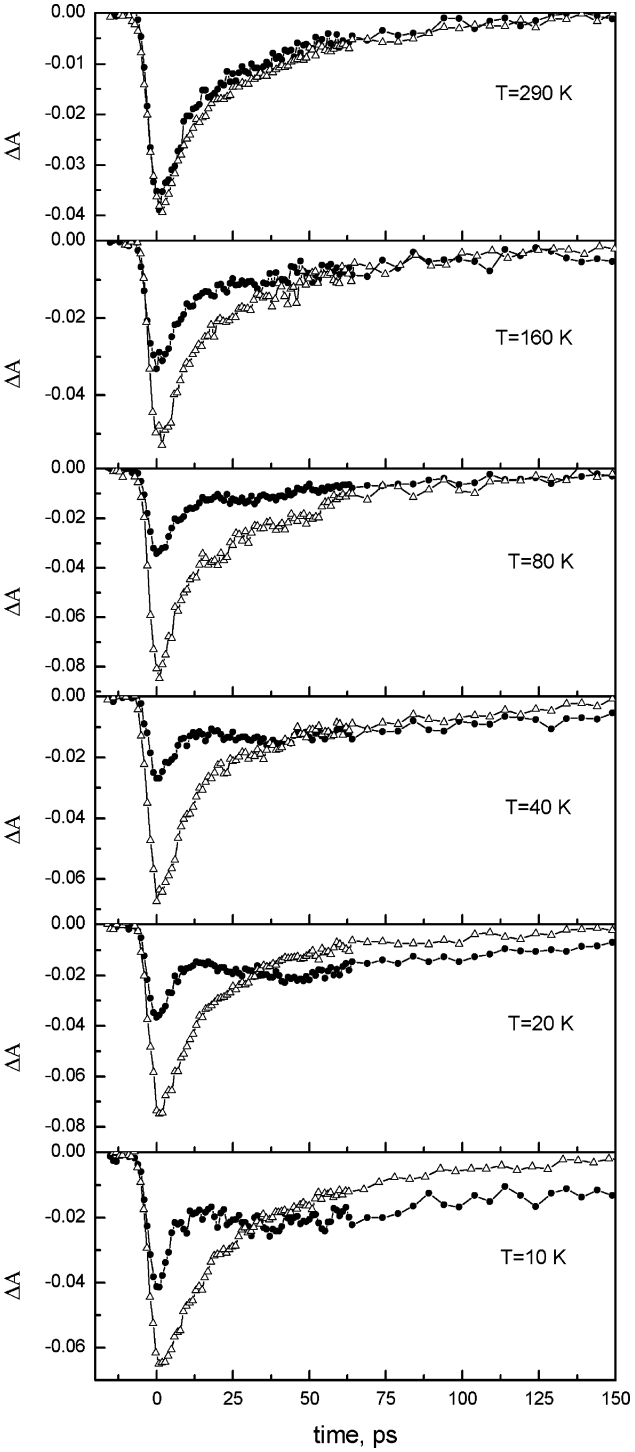

FIGURE 3: Bleaching kinetics of the LHCII aggregates at 677 (△) and 682 nm (●) at various temperatures. For excitation, the 2 ps pulses of the intensity corresponding to 36 photons/trimer were applied at 624 nm.

At low temperatures, the final stage of the exciton decay kinetics, manifested as a red shift of the bleaching band of the transient spectrum, is even slower, proceeding in tens of picoseconds. These slow kinetics can also be attributed to the exciton localization, as might be concluded from the transient spectra obtained at low excitation intensities when annihilation and local heating have a minor influence.

The spectral dynamics observed at high excitation intensities is evidently related to exciton−exciton annihilation and to successive local heating effects (*22*, *26*, *27*). Exciton−

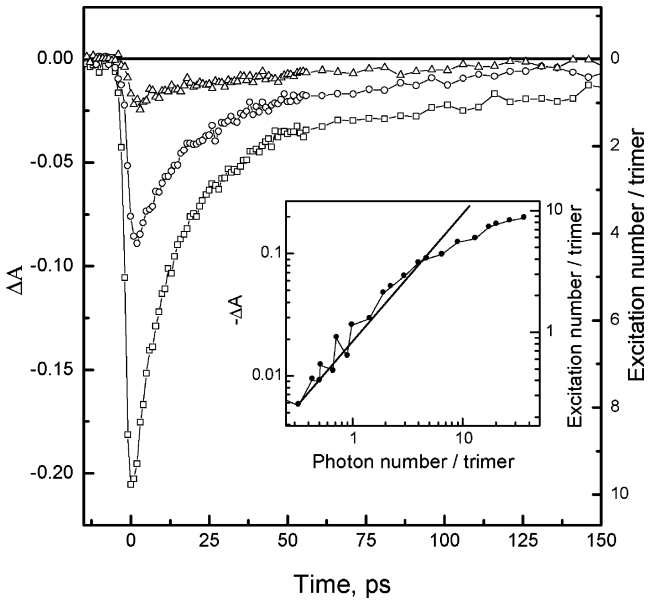

FIGURE 4: Bleaching kinetics of the LHCII aggregates at 677 nm at different excitation intensities. The measurements were carried out at 10 K. The excitation intensities of 68 photons/trimer are depicted as squares, 6 photons/trimer as circles, and 2 photons/trimer as triangles. The dependence of these values on the excitation intensity at zero delay time is shown in the inset.

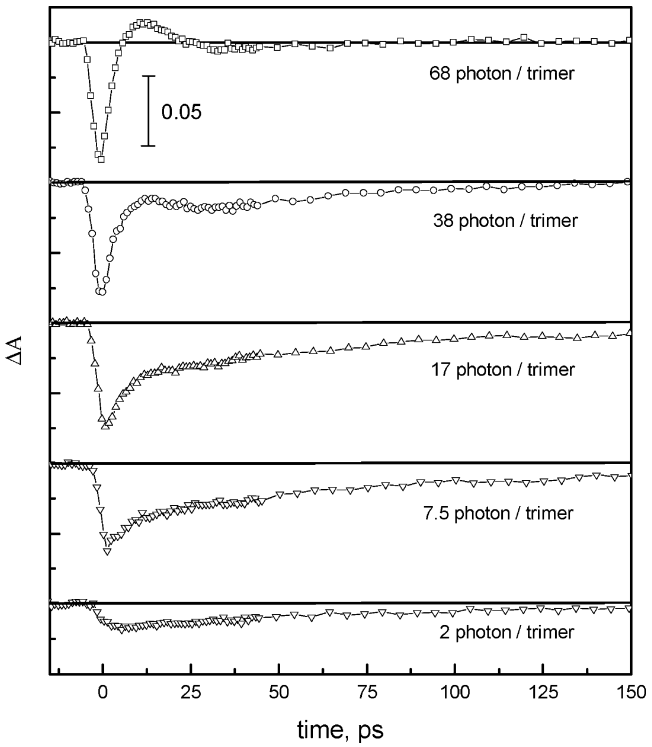

FIGURE 5: Bleaching kinetics of the LHCII aggregates at 682 nm at different excitation intensities. The measurements were carried out at 10 K. The curves are shifted along the vertical axes.

exciton annihilation results in a very fast nonradiative relaxation with a simultaneous conversion of the electronic excitation energy into heat. Therefore, the distortion of the kinetics at 682 nm at highest excitation intensities, as shown in Figure 5, can be attributed to the manifestation of the nonequilibrium (local) heating. Due to local heating, the Chl *a* absorption spectrum should broaden and shift to the long wavelength side. The heating effect vanishes during tens of picoseconds as a result of the cooling of Chl *a* molecules.

At an excitation intensity reaching ~4 excitons/trimer, the exciton density estimated at a zero delay time starts to saturate, reaching almost complete saturation at the level close to 10 excitons/trimer (see the inset of Figure 4). Therefore, we can conclude that the majority of excitons are annihilated during the pump pulse at high excitation intensities with fewer than 10 excitons/trimer, or two or three excitons in every LHCII monomer remaining after the rapid, pulse duration-limited annihilation stage. Nonlinear annihilation of the remaining excitons takes place on a much slower, reaching tens of picoseconds, time scale. According to this estimation, approximately half of the excitons are annihilated in the course of the pump pulse at the excitation intensity of 17 photons/trimer per pulse.

The resonance energy transfer from an excited molecule to the other one, which is also in the excited state, results in the transition of one of the molecules into its ground state with a simultaneous transition of the other to a higher electronic excited state. Relaxation from this higher excited state to the lowest excited state typically proceeds on a subpicosecond time scale, thus predetermining the annihilation process. As a result of this fast relaxation of the electronic excitation energy into the vibrational energy, only molecules, finally remaining in the excited state, might be locally heated after a single annihilation step. Since the bleaching band results from molecules remaining in the ground state and, thus, not heated during this step of annihilation, we do not expect to observe any noticeable heating effect in the bleaching bands. The stimulated emission spectrum, which also contributes to the bleaching band, might experience heating effects. However, the probe (682 nm) is chosen in the vicinity of the maximum of the emission band; therefore, the heating-induced changes in the emission spectrum should be negligible. Over time, the exciton is transferred from the already heated molecule to the neighboring molecules, which are in the ground state, thus, resulting in separation of heat and the electronic excitation. As a result, the effect of local heating can be expected at longer delay times. Thus, the observations with excitation intensities of 17 photons/trimer per pulse can be attributed to the local heating-induced distortion of the kinetics at 682 nm (see Figure 5).

At high excitation intensities, the excitons turn out to be involved in multiple annihilative reactions, which initiate local heating of the molecules in the ground state. Since the exciton density saturates the situation at very high excitation intensities differs from that at moderate intensities (corresponding to ~10 excitons/trimer) only by the amount of heated molecules in the ground state and by the value of their temperature reached as a result of annihilation in the course of the pump pulse. Thus, by subtracting kinetics at high and moderate intensities, we might be able to define the local heating effect on the absorption spectrum. The resultant kinetics at 682 nm is shown in Figure 6 and was obtained by subtracting kinetics at the intensity corresponding to 7.5 photons/trimer from the kinetics induced by higher-intensity excitation. Since the exciton concentration does not saturate completely at those intensities, both kinetics were equally normalized at the zero delay time before subtraction.

By comparison of stationary heating-induced spectral changes, which might be deduced from Figure 2, with the transient spectra attributed to the local heating at a 15 ps

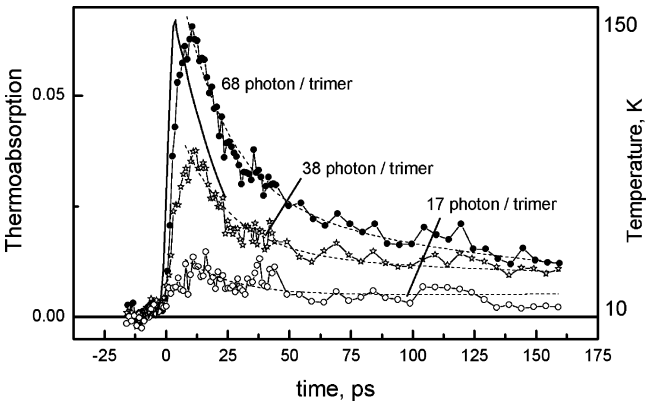

FIGURE 6: Calculated heating-induced absorption changes at 682 nm of the LHCII aggregates at 10 K for different excitation intensities. Dashed lines show curve fits with a biexponential function with 20 and 200 ps time constants. The right axis indicates the estimated local temperature. The solid line shows the calculated temperature kinetics.

delay, a qualitative similarity is obvious. Indeed, enhancement of the absorption in the 680−690 nm region and its reduction in the 660−675 nm region are obvious under both conditions. Thus, the spectral changes induced by the nonequilibrium heating are quite similar to those obtained with stationary external heating. Assuming they are equivalent, the absolute values of the local temperatures can be estimated from comparisons of the transient and stationary spectra. Values of the nonequilibrium temperature that follow from this estimation are depicted in Figure 6 (right axis).

The nonequilibrium temperature is the proper quantity for characterizing the local heating effect, and its time evolution would be determined by the flow of the heat energy to the Chl *a* molecules (as a result of exciton relaxation) and their subsequent cooling. This can be defined by the following kinetic equation for the heat−energy exchange (*22*):

$$C\frac{\mathrm{d}(T)}{\mathrm{d}t} = \Gamma(t) - \beta(T - T_0) \qquad (2)$$

where C is the thermal capacity of the Chl *a* system, T is its nonequilibrium temperature, $\Gamma(t)$ is the heat energy flow to the Chl *a* molecules, and β determines the heat loss due to the energy exchange with the bath, which is characterized by ambient temperature T_0. By assuming that the ultrafast annihilation phase and vibrational relaxation are much faster than the pulse duration, the heat flow is defined by two constituents. The first one is caused by the instantaneous energy flux that follows the Gaussian shape of the excitation pulse, and the second one taking place on the picosecond time scale is determined by the exciton relaxation kinetics (*20*, *22*):

$$\Gamma(t) = \begin{cases} A_1 \ \exp(-4 \ln 2t^2/\tau^2) & t < \tau \\ A_2 \ \dfrac{\mathrm{d}n^*}{\mathrm{d}t} & t > \tau \end{cases} \qquad (3)$$

where τ is the excitation pulse duration and n^* is the exciton number per trimer. Coefficients A_1 and A_2 are defined by the excitation intensity: if $n^* < 10$, then $A_1 = 0$ and $A_2 = 1$, and if $n^* > 10$, then $A_1 = (n^* - 10)/n^*$ and $A_2 = 1 - A_1$. Kinetics calculated according to these relations are also shown in Figure 6. The calculated temperature jump is faster than the temperature-induced spectral changes.

The red shift of the LHCII absorption band with temperature, i.e., the temperature-induced spectral changes, might be caused by either (a) population of vibrational modes (*28*), or (b) structural changes (*12*). The vibrational excitations are generated almost instantaneously as a result of relaxation from the high excited states; therefore, this process cannot explain the delay of the temperature-induced spectral changes. Thus, these temperature-induced spectral changes should be related to the structural modifications. These structural changes manifest themselves spectroscopically via pigment−pitment and pigment−protein interactions. Thermal expansion is evidently expected with an increase in temperature. Such an effect caused by the thermal expansion together with the generation of acoustic waves was observed in the picosecond transient absorption of the phthalocyanine film (*26*). The thermal expansion of the entire LHCII complex proceeds at the speed of sound, which should be on the order of 1000 m/s in liquids and organic materials. Thus, the expansion of the LHCII trimer on the order of several nanometers should proceed during several picoseconds, which is in good agreement with the thermally induced absorption kinetics described above. The spectral shift should be related to protein conformational changes (*12*) and cannot be identified with temperature-induced changes in the population of vibrational states, as suggested by analyzing the stationary spectra (*28*).

The decaying part of the temperature kinetics is obviously caused by the energy exchange with the bath, i.e., by the cooling process. As follows from experimental observations, the temperature decay is approximated well by two exponentials with time constants of ∼20 and ∼200 ps. Since the heat spreading occurs almost simultaneously, the fast cooling stage is probably even faster. A cooling time shorter than 10 ps is typical of Chl-size molecules (*29*). The excess heat energy during this time is distributed between Chl molecules through the pigment−protein complex. The slow component evidently originates from heat exchange with the solvent. The thermal diffusion coefficient in proteins (D_T) equals 7−14 Å^2/ps (*30*, *31*). Since the time scale of the heat spreading over distance L can be estimated as $L^2/(2D_T)$, 200 ps should correspond to approximately the 5−8 nm radius of heat diffusion. This is a reasonable estimation for small LHCII aggregates.

Heating values, which are a result of excitation, can be estimated from the energy balance. As follows from the comparison of heat capacity values with those of other organic molecules similar in size, the heat capacity of the Chl molecules is on the order of 1000 J mol^{-1} K^{-1} at room temperature. The molecular heat capacity should decrease with temperature, becoming approximately 2 times lower at 80 K and 10 times lower at 10 K (*32*). By using these values, the local temperature resulting from exciton−exciton annihilation can be estimated. For instance, in the case of the pump intensity of 68 photons/trimer per pulse and taking into account the fact that only 10 of the generated excitons survive after the excitation pulse, we conclude that the local temperature of all Chl molecules in the trimer should increase by 250 K at room temperature. For lower temperatures, the heating effect should give even higher values because of the decrease in the molecular heat capacity. Evidently, such a

type of estimation gives the highest possible value of the local temperature. Because of heat exchange with the protein and finally with the solvent, the local temperature would relax in time. For instance, at 10 ps when the largest absorption changes are observed, the heat energy is already partially distributed between Chl molecules and their nearest environments. Thus, the entire trimer should be in the heated condition at this time. By taking into account the heat capacity of the entire LHCII trimer, which according to the same estimation should be ~170 000 J/K, we conclude the trimer must be heated by ~70 K at room temperature at an excitation intensity of 68 photons/trimer per pulse. At low temperatures, the nonequilibrium temperature should be 2−3 times higher. These estimations are in good agreement with the estimation obtained from temperature-induced absorption changes. However, the local temperature values at room temperature are evidently overestimated because no heating-induced changes are observed in the experimental transient spectra.

CONCLUSION

It has been demonstrated that the local heating, which is strongly enhanced by exciton−exciton annihilation, is responsible for significant spectral changes in the transient spectra of the LHCII complexes under excitation. At low temperatures, the heating manifests itself as a red shift of the longest wavelength Chl *a* absorption band and starts at excitation intensities of ~10 photons/trimer per pulse. The heating estimated from transient absorption kinetics has a maximal value with an ~10 ps delay and reaches ~70 K at an external temperature of 10 K and ~70 photons/trimer per pulse. The cooling kinetics are defined well by two phases. The fast phase with the characteristic time constant of ~20 ps is related to the transfer of heat from the Chl *a* molecules to the surrounding protein. The slower phase with a time constant on the order of 200 ps should be attributed to the cooling of the entire complex.

ACKNOWLEDGMENT

Thanks to Dr. Zsuzsanna Várkonyi and Anett Kiss for the LHCII preparations.

REFERENCES

1. Allen, J. F., and Forsberg, J. (2001) Molecular Recognition in Thylakoid Structure and Function, *Trends Plant Sci. 6*, 317−326.
2. Aro, E. M., and Ohad, I. (2003) Redox Regulation of Thylakoid Protein Phosphorylation, *Antioxid. Redox Signaling 5*, 55−67.
3. Horton, P., Ruban, A. V., and Walters, R. G. (1996) Regulation of Light Harvesting in Green Plants, *Annu. Rev. Plant Physiol. Plant Mol. Biol. 47*, 655−684.
4. Li, X. P., Bjorkman, O., Shih, C., Grossman, A. R., Rosenquist, M., Jansson, S., and Niyogi, K. K. (2000) A Pigment-Binding Protein Essential for Regulation of Photosynthetic Light Harvesting, *Nature 403*, 391−395.
5. Horton, P., Wentworth, M., and Ruban, A. (2005) Control of Light Harvesting Function of Chloroplast Membranes: The LHCII-Aggregation Model for Non-Photochemical Quenching, *FEBS Lett. 579*, 4201−4206.
6. Holt, N. E., Zigmantas, D., Valkunas, L., Li, X.-P., Niyogi, K. K., and Fleming, G. R. (2005) Carotenoid Cation Formation and the Regulation of Photosynthetic Light Harvesting, *Science 307*, 433−436.
7. Barzda, V., Vengris, M., Valkunas, L., van Grondelle, R. and van Amerongen, H. (2000) Generation of Fluorescence Quenchers from the Triplet States of Chlorophylls in the Major Light-Harvesting Complex II from Green Plants, *Biochemistry 39*, 10468−10477.
8. Naqvi, K. R., Jávorfi, T., Melo, T. B., and Garab, G. (1999) More on the Catalysis of Internal Conversion in Chlorophyll *a* by an Adjacent Carotenoid in Light-Harvesting Complex (Chl *a*/*b* LHCII) of Higher Plants: Time-Resolved Triplet-Minus-Singlet Spectra of Detergent-Perturbed Complexes, *Spectrochim. Acta, Part A 55*, 193−204.
9. Van Amerongen, H., and van Grondelle, R. (2001) Understanding of Energy Transfer Function of LHCII, the Major Light Harvesting Complex of Green Plants, *J. Phys. Chem. B 105*, 604−617.
10. Jennings, R. C., Garlaschi, F. M., and Zucchelli, G. (1991) Light-Induced Fluorescence Quenching in the Light-Harvesting Chl *a*/*b* Protein Complex, *Photosynth. Res. 27*, 57−64.
11. Barzda, V., Jennings, R. C., Zucchelli, G., and Garab, G. (1999) Kinetic Analysis of the Light-Induced Fluorescence Quenching in Light-Harvesting Chl *a*/*b* Pigment−Protein Complex of Photosystem II, *Photochem. Photobiol. 70*, 751−759.
12. Pascal, A. A., Liu, Z., Broess, K., van Oort, B., van Amerongen, H., Bobert, B., Chang, W., and Ruban, A. (2005) Molecular Basis of Photoprotection and Control of Photosynthetic Light-Harvesting, *Nature 436*, 134−137.
13. Barzda, V., Istokovics, A., Simidjiev, I., and Garab, G. (1996) Structural Flexibility of Chiral Macroaggregates of Light-Harvesting Chlorophyll *a*/*b* Pigment−Protein Complex. Light-Induced Reversible Structural Changes Associated with Energy Dissipation, *Biochemistry 35*, 8981−8985.
14. Garab, G., Leegood, R. C., Walker, D. A., Sutherland, J. C., and Hind, G. (1988) Reversible Changes of Macroorganization of the Light-Harvesting Chlorophyll *a*/*b* Pigment Protein Complex Detected by Circular Dichroism, *Biochemistry 27*, 2430−2434.
15. Istokovics, A., Simidjiev, I., Lajkó, F., and Garab, G. (1997) Characterization of Light Induced Reversible Changes in the Microorganization of the Chromophores in Chloroplast Thylakoid Membranes. Temperature Dependence and Effect of Inhibitors, *Photosynth. Res. 54*, 45−53.
16. Cseh, Z., Rajagopal, S., Tsonev, T., Busheva, M., Papp, E., and Garab, G. (2000) Thermooptic Effect in Chloroplast Thylakoid Membranes. Thermal and Light Stability of Pigment Arrays with Different Levels of Structural Complexity, *Biochemistry 39*, 15250−15257.
17. Cseh, Z., Vianelli, A., Rajagopal, S., Krumova, S., Kovács, L., Papp, E., Barzda, V., Jennings, R., and Garab, G. (2005) Thermo-Optically Induced Reorganizations in the Main Light Harvesting Antenna of Plants. I. Non-Arrhenius Type of Temperature Dependence and Linear Light-Intensity Dependences, *Photosynth. Res. 86*, 263−273.
18. Dobrikova, A. G., Várkonyi, Z., Krumova, S. B., Kovács, L., Kostov, G. K., Todinova, S. J., Busheva, M. C., Taneva, S. G., and Garab, G. (2003) Structural Rearrangements in Choroplast Thylakoid Membranes Revealed by Differential Scanning Calorimetry and Circular Dichroism Spectroscopy, *Biochemistry 42*, 11272−11280.
19. Garab, G., Cseh, Z., Kovacs, L., Rajagopal, L., Varkonyi, Z., Wentworth, M., Mustardy, L., Der, A., Ruban, A. V., Papp, E., Holzenberg A., and Horton, P. (2002) Light-Induced Trimer to Monomer Transition in the Main Light-Harvesting Antenna Complex of Plants: Thermo-Optic Mechanism, *Biochemistry 41*, 15121−15129.
20. Valkunas, L., and Gulbinas, V. (1997) Nonlinear Exciton Annihilation and Local Heating Effects in Photosynthetic Antenna Systems, *Photochem. Photobiol. 66*, 628−634.
21. Simidjiev, I., Barzda, V., Mustárdy, L., and Garab, G. (1997) Isolation of Lamellar Aggregates of the Light-Harvesting Chlorophyll *a*/*b* Protein Complex of Photosystem II with Long-Range Chiral Order and Structural Flexibility, *Anal. Biochem. 250*, 169−175.
22. Van Amerongen, H., Valkunas, L., and van Grondelle, R. (2000) *Photosynthetic Excitons*, World Scinetific Co., Singapore.
23. Becker, M., Nagarajan, V., and Parson, W. (1991) Properties of the Excited-Singlet States of Bacteriochlorophyll *a* and Bacteriopheophytin *a* in Polar Solvents, *J. Am. Chem. Soc. 113*, 6840−6848.
24. Gradinaru, C. C., Ozdemir, S., Gülen, D., Stokkum, I. H. M., van Grondelle, R., and van Amerongen, H. (1998) The Flow of Excitation Energy in LHCII Monomers: Implication of the Structural Model of the Major Plant Antenna, *Biophys. J. 75*, 3064−3077.

25. Barzda, V., Gulbinas, V., Kananavicius, R., Cervinskas, V., van Amerongen, H., van Grondelle, R., and Valkunas, L. (2001) Singelt-Singlet Annihilation Kinetics in Aggregates and Trimers of LHCII, *Biophys. J. 80*, 2409−2421.
26. Butvilas, V., Gulbinas, V., Urbas, A., and Vachnin, A. J. (1992) Ultrafast Processes in VO-Phthalocyanine Film Caused by Intense Excitation, *Radiat. Phys. Chem. 39*, 165−169.
27. Gulbinas, V., Valkunas, L., and Gadonas, R. (1994) Exciton annihilation and local heating in molecular aggregates, *Lith. J. Phys. 34*, 348−360.
28. Zucchelli, G., Garlaschi, F. M., and Jennings, R. C. (1996) Thermal Broadening Analysis of the Light Harvesting Complex II Absorption Spectrum, *Biochemistry 35*, 16247−16254.
29. Okazaki, T., Hirota, N., and Terazima, M. (1999) Thermalization Process after the Relaxation of Electronically Excited States: Intramolecular Proton Transfer Systems Studied by The Transient Grating Method, *J. Chem. Phys. 110*, 11399−11410.
30. Tesch, M., and Schulten, K. (1990) A Simulated Cooling Process for Proteins, *Chem. Phys. Lett. 169*, 97−102.
31. Yu, X., and Leitner, D. M. (2003) Vibrational Energy Transfer and Heat Conduction in a Protein, *J. Phys. Chem. B 107*, 1698−1707.
32. Crawford, F. H. (1963) *Heat, Thermodynamics and Statistical Physics*, Harcourt, Brace and World, Inc., New York.

BI060048A